General Disclaimer

One or more of the Following Statements may affect this Document

- This document has been reproduced from the best copy furnished by the organizational source. It is being released in the interest of making available as much information as possible.

- This document may contain data, which exceeds the sheet parameters. It was furnished in this condition by the organizational source and is the best copy available.

- This document may contain tone-on-tone or color graphs, charts and/or pictures, which have been reproduced in black and white.

- This document is paginated as submitted by the original source.

- Portions of this document are not fully legible due to the historical nature of some of the material. However, it is the best reproduction available from the original submission.

Produced by the NASA Center for Aerospace Information (CASI)

JSC-13985

(NASA-TM-79741) IMPINGEMENT EFFECT OF SERVICE MODULE REACTION CONTROL SYSTEM ENGINE PLUMES. RESULTS OF SERVICE MODULE REACTION CONTROL SYSTEM PLUME MODEL FORCE FIELD APPLICATION TO AN INFLIGHT SKYLAB G3/20

N78-32180

Unclas
29939

Impingement Effect of Service Module Reaction Control System Engine Plumes

Results of service module reaction control system plume model force field application to an inflight Skylab mission proximity operation situation with the inflight Skylab response.

April 1978

NASA
National Aeronautics and Space Administration

Lyndon B. Johnson Space Center
Houston, Texas

IMPINGEMENT EFFECT OF SERVICE MODULE REACTION CONTROL SYSTEM ENGINE PLUMES

RESULTS OF SERVICE MODULE REACTION CONTROI SYSTEM PLUME MODEL FORCE FIELD APPLICATION TO AN INFLIGHT SKYLAB MISSION PROXIMITY OPERATION SITUATION WITH THE INFLIGHT SKYLAB RESPONSE

PREPARED BY

John D. Lobb, Jr.
Engineering Evaluation Analysis Office

APPROVED BY

D. D. Arabian
Manager, Program Operations

NATIONAL AERONAUTICS AND SPACE ADMINISTRATION

LYNDON B. JOHNSON SPACE CENTER

HOUSTON, TEXAS

April 1978

TABLE OF CONTENTS

Section	Page
SUMMARY	1
INTRODUCTION	3
PRE-DOCKING FLY-AROUND INSPECTION	4
PLUME IMPINGEMENT MODEL	5
PLUME IMPINGEMENT ON SATURN WORKSHOP PARASOL	6
PLUME IMPINGEMENT ON SATURN WORKSHOP SOLAR ARRAYS	7
DATA	8
CONCLUSIONS	14
REFERENCES	15

LIST OF TABLES

TABLE I.- INDUCED NEGATIVE ROLL BASED ON PLUME MODEL AND SPACECRAFT DATA	9
TABLE II.- POSITIVE ROLL RESPONSE - BASED ON SATURN WORKSHOP DATA	10
TABLE III.- SKYLAB 3 ANALOG DATA BILEVEL STRIP CHART RECORDS	13

LIST OF FIGURES

1.- Saturn workshop thruster attitude control system and service module reaction control system thruster identification	16
2.- Predocking approach and fly-around on second visit to Skylab	
(a) Proximity operations	17
(b) Notes for figure 2	18
3.- Spacecraft, workshop and parasol during approach and fly-around maneuver	19

4.- Command and service module reaction control system plume impingement model 20

5.- Workshop parasol in plume impingement model force fields for service module reaction control system thrusters A-3 and C-4 at about 209:19:14.33 G.m.t. 21

6.- Saturn workshop solar arrays in plume impingement model force fields for reaction control system thrusters A-3 and C-4

(a) Spacecraft/workshop separation distance of 100 feet 22

(b) Spacecraft/workshop separation distance of about 200 feet . . 23

(c) Spacecraft/workshop separation distance of about 265 feet . . 24

7.- Saturn workshop parasol at 209:19:14.33 G.m.t. 25

8.- Finding workshop - spacecraft separation distances 26

9.- Finding attitude orientation angles between the spacecraft and workshop 27

10.- Dynamic pressure

(a) At parasol 28

(b) From plume impingement model 29

11.- Saturn workshop dimensions 30

SUMMARY

During the Shuttle Payloads proximity operations of rendezvous, retrieval and deployment, the Shuttle payloads will be subject to the effects of possible impingement forces from the Orbiter reaction control systems plumes. Therefore, the plume effects must be understood so that appropriate countermeasures are provided through flight mechanics, flight procedures, and design of the payloads and payload interfaces.

The plume model being used in the Shuttle engineering simulator and other premission activities was generated with source flow plume impingement program techniques equivalent to those used for the Apollo service module reaction control system plume impingement analyses for the proximity operations in the Skylab program. Agreement between Skylab flight experience and the service module reaction control system plume impingement model could validate at least part of the Orbiter reaction control system plume model.

Determining the effect of plume impingement during proximity operations was not an objective on any Skylab mission and, consequently, data were not collected nor processed for proximity operations studies; however, the analog and bilevel telemetry data, television data and voice downlink data obtained during the command and service module pre-docking approach and fly-around at the beginning of the second visit to Skylab provided data for analysis of proximity operations. In addition, the nearly complete coverage obtained with the 16-mm data acquisition camera onboard the command module provided usable data for the study. The digital data that made up the majority of the Skylab data were not available for this study because changes in the ground stations hardware and software since the completion of the Skylab program deleted the capability to process the Skylab digital data.

The approach and fly-around profile was determined from the 16-mm photography, television, and time-annotated voice transcripts. The flapping canopy on the Saturn Workshop parasol was observed in a film sequence photographed at 209:19:14:33 G.m.t., from which measurements were made to determine the size and shape of the flapping corner, the distance moved, and the rate of movement. These data were used to calculate the actuating force using simple force equations.

The distance and pointing angles from the service module reaction control system to the parasol flap were also determined from the photography. These data and the plume-model profile of dynamic pressure versus distance from the service module thrusters were used to calculate the force on the flap using the plume model.

Agreement between the force equation and plume-model-derived results for the two flapping actions of a corner of the lightweight parasol canopy was good: For the smaller flapping action, the force equation results were 0.574 lb compared to 0.602 lb from the plume model. For the larger flapping action, the force was 1.207 lb from the force equations compared to 1.346 lb from the plume model.

The use of the forward-firing service module thrusters A-3 and C-4 during the approach and beginning of the fly-around also placed a force on the Saturn Workshop solar arrays that induced a negative roll moment on the workshop. The photographic data, analog data, plume impingement model, and the workshop geometry were used to determine the force on the solar arrays and the induced negative roll moments on the workshop. For comparison, previously evaluated Saturn Workshop flight data were used to determine the positive roll torque and moment developed by the workshop thruster attitude control system firings in response to the torques and moments induced by the service module reaction control system plume impingement on the solar arrays.

Agreement between the calculated results was good for the roll stabilization of the workshop. The results were a positive roll response of 4235 ft-lb-sec by the thruster attitude control system compared with 3369 ft-lb-sec negative roll induced by the service module thrusters using the plume impingement model.

On the basis of the measurements and calculations, good agreement exists between the source flow plume impingement program model for the service module reaction control system thrusters and the Skylab flight experience for the separation distances and angles evaluated.

INTRODUCTION

The study of the plume impingement effects of the service module reaction control system thruster firings was initiated to determine if previous flight experience would support the current plume impingement model for the orbiter reaction control system engines. The orbiter reaction control system is used for rotational and translational maneuvers such as those required during rendezvous, braking, docking, and station-keeping. Therefore, an understanding of the characteristics and effects of the plume force fields generated by the reaction control system thruster firings is required to develop the procedures for orbiter/payload proximity operations.

Current orbiter/payload proximity-operation studies and the Shuttle engineering simulator have made use of the plume models developed by both the source flow plume impingement program and a plume impingement program that uses the method of characteristics to determine the plume flow field. Agreement between the two programs has been good over the range of force field angles and distances that apply to this study. Although the orbiter reaction control system engines differ significantly from the Apollo service module reaction control system engines in size, shape and performance, the source flow plume impingement program plume model techniques are applicable to both the orbiter and the service module engines. The method of characteristics plume and plume impingement program model for the service module reaction control system thruster plume was used in developing the Apollo, Skylab, and Apollo Soyuz Test Project rendezvous and docking procedures. In each of these previous spaceflight programs, the flight procedures were based on the predicted effects of the reaction control system plumes and were satisfactory with good control being maintained.

Determining the effect of plume impingement during proximity operations was not an objective for any of the Apollo, Skylab, or Apollo-Soyuz Test Project missions, rather the operational procedures were developed to avoid, not explore such effects. Data were not collected nor processed for proximity-operation studies, but a command and service module pre-docking fly-around inspection of the Saturn Workshop on the second Skylab visit did provide the only usable flight data on plume impingement in a proximity operation situation. In fact, the fly-around was terminated early, and future fly-arounds avoided because of the visible effect of the service module reaction control system plumes on the thermal protection parasol that had been installed on the workshop during the first Skylab visit. The parasol fabric canopy flapped vigorously in the force field generated within the reaction control system thruster plumes.

The study covered by this report was based on the fly-around experience of the second Skylab visit. Although available flight data were limited, as stated previously and discussed in the Data Section, the comparisons performed between values calculated from flight experience and those calculated from plume models were in two categories:

a. Plume impingement on the parasol fabric canopy with an impingement surface-to-canopy body-weight ratio of about 90:1.

b. Plume impingement on the workshop solar array panels with an impingement-surface-to-workshop body-weight ratio of about 12:1000.

PRE-DOCKING FLY-AROUND INSPECTION

Prior to the fly-around maneuver by the spacecraft, the service module reaction control system quads B and D (fig. 1) were disabled for plus or minus X translations because of a problem with quad B. As a result, the forward-firing thrusters A-3 and C-4 were used for braking as the spacecraft neared the workshop and thus were the source of plume impingement on the workshop.

Approach to the Saturn Workshop with the manned command and service module was from below, viewing the -Z underside of the workshop against the dark background of deep space (fig. 2). The workshop first appeared in the field of view of the 16-mm data acquisition camera at a distance of about 1200 feet. At a distance of about 165 feet (fig. 3), some motion of the parasol (see section on Plume Impingement on Saturn Workshop Parasol) was observed in the 16-mm photography. Although the parasol was mounted on the +Z scientific airlock, parasol motion was sometimes visible from the -Z side because the workshop was rolled approximately 26° clockwise, a position that roughly aligned the camera with the workshop wardroom window.

The approach ended at a distance of about 137 feet, and the command and service module moved along in the +X direction of the workshop around the docking ring, and to the +Z side of the workshop. There the +Z (top-side) of the workshop was viewed with the sunlit earth in the background. As the parasol came into the field of view of the camera, parasol canopy flapping was observed at a distance of about 160 feet. The fly-around was terminated because of the excessive flapping of the parasol as the distance decreased to about 134 feet.

As the spacecraft was backed away from the workshop to begin the docking sequence, maneuvers to minimize plume impingement resulted in spacecraft attitudes that prevented continuous photography of the parasol. The spacecraft was closest to the workshop while passing along the -Z underside of the multiple docking adapter portion of the workshop.

The fly-around profiles in figures 2 and 3 were derived from measurements and observations made from the motion picture film (ref. 1), video tapes (ref. 2), and time-annotated air-ground voice transcripts (ref. 3). The measurements and calculations are discussed further in the Data section of this report.

Two flapping motions of the forward right-hand portion of the parasol canopy (209:19:14:33 G.m.t.) were the only sequences of the 16-mm film in which the rate of motion of the parasol canopy was within the frame-rate resolution of the film, and where the view angle presented measurable parasol configuration elements in each frame. These two flaps of the parasol canopy and the effect of plume impingement on the fabric canopy are discussed in the section of the report on Plume Impingement On The Saturn Workshop Parasol.

Counterclockwise roll torques were induced on the workshop by service module reaction control system thruster plume impingement on the solar arrays when the spacecraft approached the -Z underside of the workshop at the start of the fly-around. The workshop had previously been placed in the nominal momentum cage

mode for stabilization and control. In this mode, the gravity-gradient attitude was maintained by the control moment gyros and the reactions caused by events such as vent dumps and plume impingement were stabilized by thruster attitude control system firings. No vent dumps occurred during the approach and fly-around period, therefore, the firing commands to the thruster attitude control system were to negate the effects of the service module reaction control system thruster plume impingement and thereby maintain workshop stabilization. The workshop roll effect from reaction control system thruster plume impingement on the solar array is discussed in more depth in that section of the report.

PLUME IMPINGEMENT MODEL

The service module reaction control system plume model used was developed for a desktop calculator and was based on the source flow plume impingement program (ref. 4), instead of the method of characteristics plume flow plume impingement program that was utilized on the Apollo, Skylab, and Apollo-Soyuz test programs. Studies have shown that a source flow plume can approximate the plume flow described by the method of characteristics quite satisfactorily in the plume far field (where the distance between the thruster and impinged surface is greater than ten times the exit diameter of the thruster nozzle) and under vacuum or near vacuum conditions. The shortest distance between the service module reaction control system nozzles (exit diameter about 5.5 in.) and the workshop during the fly-around was over 90 feet, a distance that is well into the far field.

The lines of constant dynamic pressure for the plume force field in figures 4, 5, and 6, were generated on the basis of the source flow plume impingement program to a distance of over 300 feet for this study. Although single-plane two-dimensional conditions are indicated in figures 5 and 6, calculations of the effects of the plume dynamic pressures on the workshop parasol and solar arrays included the three-dimensional considerations.

The limiting turning angle, θ_ℓ, for the gas was assumed to be $\pi/2$ radians because of the relative positions of the workshop and spacecraft during the approach and fly-around sequence. The variable specific heat ratio, γ, was approximated by a constant specific heat ratio of 1.28 for the monomethyl hydrazine/nitrogen tetroxide bipropellant.

The source flow plume impingement program provided a reasonably accurate basis for the comparison of the service module reaction control system plume impingement model and the Skylab flight data. Similar techniques with the plume impingement program were used to generate the orbiter reaction control system plume impingement model. Although the propellants were the same, differences between the orbiter and service module reaction control system engines were recognized, i.e., total thrust 900 lb versus 90 lb, expansion ratio 22:1 versus 40:1, and mounting internal to moldline and shaped to fit versus external mounting.

PLUME IMPINGEMENT ON SATURN WORKSHOP PARASOL

A 25-foot by 23-foot laminated fabric parasol (fig. 7) was attached to the workshop through the +Z scientific airlock on the first manned visit. This parasol thermally protected that portion of the +Z side that was uncovered when the micrometeoroid shield was lost during the Skylab launch. The 16-mm photography taken from the command module during the pre-docking approach and fly-around maneuver on the second visit (ref. 1), showed part or all of the parasol's flexible canopy flapping vigorously from service module reaction control system thruster plume impingement whenever the spacecraft was within about 160 feet of the workshop (figs. 2, 3, 5). Some portion of the parasol was in the field of view of the camera about half the time during the photographic coverage from 209:19:03:30 G.m.t. to 209:19:19:00 G.m.t., and parasol motion was observed about 70 percent of the time when the parasol was in view. Selection of a usable frame sequence to measure parasol motion was difficult because of the unfavorable relationships between parasol motion and camera view angle and camera frame rate. However, at 209:19:14:33 G.m.t., a sequence covering two flapping motions of the forward corner of the parasol (figs. 5 and 7) was usable.

The size and shape of the flapping forward corner, the motion rates, and distances moved during the sequence were determined from the 16-mm photography, as was the separation distance and attitude relationship between the workshop parasol and the service module reaction control system thrusters (figs. 8 and 9).

Plume Model Calculations of Force on Parasol Corner

The parasol motion measurements established the position of the parasol in the force field of the service module reaction control system thruster plume model (figs. 5 and 10). The force on the parasol corner for the two flapping motions was as follows:

Thruster	Smaller flap	Larger flap
A-3 plume dynamic pressure, lb/ft^2	0.00455	0.00446
C-4 plume dynamic pressure, lb/ft^2	0.00298	0.00302
Combined force, lb	0.602	1.346
Canopy area of flapping motion, ft^2	80	180

Force Equation Calculations on Parasol Corner

The parasol canopy was an assembly of nine strips of GT-76 Nylon rip-stop cloth that was laminated with aluminized Mylar. Each strip measured 2.5 feet by 25 feet, and when sewn together, the nine strips formed the 23-foot by 25-foot canopy, and weighed about 0.177 ounce/ft^2. Stiffness of the canopy material was determined by ground tests that were required for design of the deployment and unfolding mechanical design (ref. 5). Nomex tape reinforced the canopy edge, and Polybenzimadazole cording formed attaching loops at the four corners.

The canopy was supported by four telescoping rods (fig. 7) that were attached to the corner loops by Polybenzimadazole cord. These forward two rods were not fully deployed on the first visit, allowing considerable slack and freedom for parasol flapping (ref. 6). The possibility of canopy support-tube deflections having an effect on the flapping characteristics of the canopy was recognized, and the results of the tube deflection ground tests were considered. However, no appreciable tube-deflection effects were apparent in the photography of the flapping sequence at 209:19:14:33 G.m.t.

The size, shape, distances, and rates were applied to simple force equations for the lifting and rotating movement observed; and the results of the stiffness tests were applied to the canopy seams, edge seams, and unseamed material to determine the bending forces involved in the flapping actions. The total force required to produce the measured movement of the flapping parasol corner observed in the photography was as follows:

	Smaller flap	Larger flap
Lifting force, lb	0.248	0.703
Rotating force, lb	0.307	0.481
Bending force, lb	0.019	0.023
Total, lb	0.574	1.207

Comparison

A comparison of the results of force equation calculations with the results of the plume model calculations showed reasonably good agreement.

	Smaller flap	Larger flap
Force equations, lb	0.574	1.207
Plume model, lb	0.602	1.346

PLUME IMPINGEMENT ON SATURN WORKSHOP SOLAR ARRAYS

As the spacecraft approached the -Z side of the workshop to begin the fly-around (figs. 2 and 3), the forward-firing reaction control system thrusters, A-3 and C-4 (fig. 1) that were used for braking impinged on the panels of the workshop solar array and Apollo telescope mount solar array (fig. 6) and induced a negative roll torque on the workshop. The workshop thruster attitude control system responded to the external forces by firing positive roll thrusters 3 and [illegible] (fig. 1) to maintain the desired workshop orientation. These data were determined from a selected 5-minute period of data beginning at 209:19:05 G.m.t.

At the time of the approach and fly-around, the workshop was in an attitude control mode in which the control moment gyro's maintained the workshop in the gravity gradient attitude and the thruster attitude control system was being used to maintain stability control in regard to the effect of external disturbances. However, with no crew onboard and no venting occurring, the only significant disturbances requiring thruster attitude control system operation were from the service module reaction control system thruster plume impingement.

Induced Negative Roll Determined by Plume Model

The separation distances and pointing relationships between the workshop solar arrays and the service module reaction control system thrusters during the approach and fly-around were determined. These measurements established positions of the solar arrays in the force field of the reaction control system plume model (fig. 6). The calculated values of the negative roll torque, table I, induced by the service module reaction control system thrusters A-3 and C-4 during the 5-minute period were based on the plume model dynamic pressures, service module reaction control system thruster firing times from the recorded analog data (ref. 7), and the 16-mm photography.

Positive Roll Response Determined From Saturn Workshop Data

The positive roll response (table II) from the firings of the workshop thruster attitude control system thrusters was calculated on the basis of the average rate gyro output data (ref. 8), the impulse usage required (ref. 9), and the workshop dimensions (fig. 11). The analog thruster attitude control system bilevel data (ref. 7) were invalid during this time period and could not be used to determine thruster firing times.

Comparison

A comparison of the results of the positive roll torque based on calculations from the workshop thruster attitude control system data with the negative roll torque based on plume impingement model calculation showed reasonably good agreement with a positive roll torque of 3369 ft-lb-sec and a negative roll torque of 4235 ft-lb-sec.

DATA

Availability of Data

The Skylab missions produced a vast amount of recorded data, much of which has been used in engineering analyses as well as extensive scientific analyses. During the intervening years since the completion of the last Skylab mission, February 8, 1974, and the beginning of this study, the computer-compatible master tapes have been archived, i.e., stored and made available upon request

TABLE I - INDUCED NEGATIVE ROLL BASED ON PLUME MODEL AND SPACECRAFT DATA

Time from 209:19 G.m.t., min:sec	Workshop solar array	Apollo telescope mount solar array		Induced roll in workshop and telescope mount, ft-lbs	Average induced roll, ft-lbs	Thruster A3/C4 on times, seconds	Induced torque, ft-lb-sec
	$-M_{OWS}$ (1) (Negative roll) ft-lbs	$-M_{ATM}$ (2) (Negative roll), ft-lbs	$+M_{ATM}$ (3) (Positive roll), ft-lbs				
5:00 to 6:00	42.8	26.8	(4)	69.6	92.95	14.5	1340
6:00 to 7:30	72.5	43.8	(4)	116.3	190.2	2.45	455
7:30 to 8:00	142.5	202.0	80.4(5)	264.1	248.05	2.85	709
8:00 to 9:00	139.0	157.5	64.5(5)	232.0	142.7	3.4	488
9:00 to 10:00	41.0	67.5	55.1	53.4	31.05	0.1	377
TOTAL	6.6	11.2	9.1	8.7			—
							3369

NOTES:

1. Negative roll induced by service module A3 and A4 thruster plumes impinging on workshop solar array (fig. 1).
2. Same as note 1 except on Apollo telescope mount solar arrays 1 and 4 (fig. 1).
3. Same as note 1 except for positive roll and on Apollo telescope mount solar arrays 2 and 3 (fig. 1).
4. Orientation such that Apollo telescope mount solar arrays 2 and 3 were in shadow.
5. Orientation such that Apollo telescope mount solar array 3 was in shadow.

TABLE II - POSITIVE ROLL RESPONSE - BASED ON SATURN WORKSHOP DATA

Time after 209:19 G.m.t., min:sec	P_{TACS}(1) (Positive roll) attitude rate, deg/sec	I_{TACS}(2) (Impulse) usage, lb-sec	R_{TACS}(3) (Moment arm), ft	$+M_{TACS}$(4) (Positive roll) response, ft-lb-sec
5:00 to 6:00	0.06	65	11	715
to 8:00	0.06	65	11	715
to 10:00	0.24	255	11	2805
TOTAL				4235

NOTES:

1. P_{TACS} - Positive roll attitude rate from average rate gyro output data (ref. 8).
2. I_{TACS} - Thruster attitude control system impulse usage for measured attitude rates (ref. 9).
3. R_{TACS} - Thruster attitude control system nozzles 3 and 5 roll moment arm.
4. $+M_{TACS}$ - Positive roll response from thruster attitude control system firings.

for additional analysis requirements. However, the hardware and software of the compatible computer data processing centers at Johnson Space Center and Marshall Space Flight Center have been changed to accommodate the Space Transportation System programs. Consequently, the Skylab-recorded digital data can no longer be reduced by the two ground stations.

To process the digital data, new programs that are compatible with the existing ground stations would have to be written and verified, or new ground station hardware and software that is equivalent to the previously compatible configuration would have to be built. Neither of these options were within the scope of this study or justifiable from a cost standpoint, since special programs were still available at Johnson Space Center to process some of the Skylab analog data. These programs were used to produce bilevel strip chart records of the service module reaction control system and workshop thruster attitude control system firing times during the approach and fly-around period covered by this study.

The analog data were subject, of course, to the common problems of occasional data dropouts and excessive noise. Some of the service module reaction control system thruster firing analog bilevel data were invalid because of data dropouts. Almost all of the workshop thruster attitude control system thruster firing analog bilevel data were invalid during the approach and fly-around because noise masked the data.

Although no studies were made of plume impingement effects during the approach and fly-around proximity operations, some fringe data that were applicable to this study appeared in the post flight evaluation documentation of the Saturn Workshop Attitude Pointing Control System (ref. 8).

Photographic Data

The 16-mm film taken from the command module during the approach and fly-around was used for film image measurements to calculate the spacecraft-workshop separation distances and determine the location and orientation of the workshop in the force field of the plumes from the service module reaction control system thrusters.

Coordination between the 16-mm film, the television video tape record, and the time-annotated air-ground voice transcripts provided timing for the situations observed and studied. Figure 8 shows the method used to determine the spacecraft-workshop separation distances. The method applied simple trigonometry to the combination of known camera characteristics, size of workshop elements (diameters), and film image measurements to find the distance from the camera to the workshop. An additional 8 feet was added to the calculated distance between the workshop and the camera to arrive at the service module reaction control system thrusters A-3 and C-4 positions, that are about 8 feet behind the camera location in command module window.

Figure 9 shows the method used in the calculation of the attitude-orientation pointing-angle between the command and service module and the Saturn Workshop.

Two points were selected on the workshop where the diameters were known, the distance between the points was known, and the points were measured on the 16-mm film. The angle was then determined.

Using the methods described in the previous paragraphs, distances and angles were measured from the photography, calculated, and plotted at about 50 different positions in the approach and fly-around sequence.

Figure 10, as well as figures 5 and 6, indicates the location and orientation of the workshop in the plume force field and from these data, a determination of the dynamic pressure on the parasol and on the workshop solar arrays was made. In laying out plume patterns, adjustments were made for the 10° cant angle for the A-3 and C-4 thrusters, and for the offset from the camera axis to the A-3 thruster (approximately 3.5 feet), and to the C-4 thruster (approximately 10.3 feet).

Parasol movements and flap sizes were calculated in a similar manner from known dimensions and measurements of images on the 16-mm film.

Recorded Data

The spacecraft analog data tapes were processed to provide bilevel strip charts of the service module reaction control system thruster firings (ref. 7). The data for all 16 thrusters (table III) were reviewed, confirming the inactivity of quads B and D and showing that most of the activity during the approach and fly-around was with the forward-firing thrusters, A-3 and C-4. The accumulated A-3 and C-4 thruster time data for the selected time period were used in the calculation of accumulated negative roll torque induced by plume impingement on the solar arrays.

Documented Data

Digital data were processed for the post flight evaluation of the workshop/orbital assembly attitude pointing control system, and portions of these data were presented in some of the figures in the evaluation report (ref. 8) to support the discussion of the docking operation on the second visit. In some of these plots of the flight data, the time period covering the approach and fly-around was included with the docking sequence. As a result, the average rate gyro output data were available for this study as fringe data from the attitude pointing control system evaluation documentation. These data were used in determining the workshop positive roll response.

Documented data for the workshop thruster attitude control system impulse usage rate to maneuver the workshop was provided by the Operational Data Book (ref. 9). These data were also used in determining the workshop positive roll response.

The service module reaction control system plume model used and discussed in the report on the plume impingement model was generated on the basis of the source flow plume impingement program (ref. 4).

TABLE III - SKYLAB 3 ANALOG DATA BILEVEL STRIP CHART RECORDS[1]

(a) Spacecraft PCM Bilevel Tabulation[2]

Chart track[3]	Reaction control system thruster	Solenoid actuator measurement no.	Loading no. high bit rate bit	Chart track	Reaction control system thruster	Solenoid actuator measurement no.	Loading no. high bit rate bit
1	C3	CH3546-X	2201018A12	1	B1	CH3554-X	2201019A12
2	A3	CH3548-X	2201018C12	2	D1	CH3556-X	2201019F12
3	A4	CH3547-X	2201018B12	3	D2	CH3555-X	2201019E12
4	C4	CH3549-X	2201018D12	4	B2	CH3557-X	2201019B12
5	D3	CH3550-X	2201018E12	5	A1	CH3558-X	2201019G12
6	B3	CH3552-X	2201018G12	6	C1	CH3560-X	2201019D12
7	B4	CH3551-X	2201018F12	7	C2	CH3559-X	2201019C12
8	D4	CH3553-X	2201018H12	8	A2	CH3561-X	2201019H12

(b) AM-1 Saturn Workshop RF Link[2]

Chart track[3]	Thruster attitude control system thruster	Pressure switch measurement no.	Identification		
			Frame	Word	Bit
1	3	K 7030-404	03	094	1
2	1	K 7031-404	03	094	2
3	2	K 7032-404	03	094	3
4	5	K 7033-404	03	094	4
5	4	K 7034-404	03	094	5
6	6	K 7035-404	03	094	6

NOTES:

1. The data were received at 51.2 kbps in an 8-bit word format and were processed in the Johnson Space Center on the Special Telemetry Conversion System/Vector System and printed at a chart speed of 50 mm/sec.

2. The G.m.t., the tape no., and the ground station that received the data that were processed were as follows:

   -209:19:04:47 to 209:19:11:10 G.m.t. - Tape no. Z05-000015 - Goldstone
   -209:19:12:40 to 209:19:20:30 G.m.t. - Tape no. Z05-000016 - Bermuda, except for the period from 209:19:16:20 to 209:19:18:20 when a data dropout occurred and no data were present on the tape.

3. In addition to the data processed, the pulse code modulation sychronization status and G.m.t. were also shown on the strip chart records.

ORIGINAL PAGE IS
OF POOR QUALITY

Other Sources of Information

The Skylab best estimate trajectory (SKYBET) data tabulations and prints of time history reports in formatted tabs (THRIFT) near-real-time data were examined as possible sources of information. Although too gross in resolution and sample rate, the discernible events and trends confirmed the results of the study.

The workshop dimensions that were used (fig. 11) were collected from many Skylab project documents, including handbooks, reports, data books and drawings. Parasol characteristics were provided by construction drawings and test reports (ref. 6).

In addition, flight control logs, flight controllers, subsystem specialists, and flight crew members were consulted and contacted for additional details, clarification, and personal observations.

CONCLUSIONS

Good agreement exists between the study results using Skylab flight data, and the results using the source flow plume impingement program model for the service module reaction control system.

Techniques used in the generation of source flow plume impingement program models are acceptable, based on the agreement of study results using Skylab flight data, and results using the afore stated plume impingement model for the service module reaction control system.

The agreement between the applications of Skylab flight data and the source flow plume impingement program model for the service module reaction control system was true for the impingement forces lifting a part of a lightweight parasol canopy on the Saturn workshop, and also for the impingement forces on the solar arrays inducing rolling moments on the heavier Saturn workshop.

Plume impingement from the forward-firing spacecraft thrusters (A-3, C-4) caused movement of the workshop parasol canopy from as far away as 165 feet.

Plume impingement forces from the forward-firing service module reaction control system thrusters A-3 and C-4 against the solar array panel surfaces during the approach and fly-around from about 265 feet to about 100 feet separation distance was sufficient to induce negative roll moments on the workshop thus causing the workshop thruster attitude control system to respond.

Future retrieval and processing of Skylab digital data will require either new programming that will be compatible with the stored data and with the present ground station, or changes to the present ground station to make the station compatible with the stored data.

REFERENCES

1. Skylab SL-3 Data Acquisition Camera 16-mm Operational Film, Reel A-112, Fly-Around Activity. 1973. NASA, JSC, Houston, Texas.

2. Skylab SL-3 Onboard Television Video Tape No. SL3-5. 1973. NASA, JSC, Houston, Texas.

3. Skylab 1/3 Technical Air-To-Ground Voice Transcription. JSC-08476 Part I, JSC Technical Library No. T73-18638, October, 1973. Prepared by Test Division, Program Operations Office, L. B. Johnson Space Center, Houston, Texas. Goldstone Pass 209:19:04:35 through 10:53 (pages 5 of 9/51 through 7 of 9/53), and Bermuda Pass 209:19:12:33 through 19:43 (pages 7 of 9/53 through 9 of 9/55). Tag Tape 209-08/T-6.

4. Kanipe, David B. Description of a Computer Program, Written for the HP Model 9830 Calculator, to Calculate Plume Impingement Forces and Moments on Surfaces Immersed in a Rocket Exhaust Plume. JSC-10891. NASA, JSC, Houston, Texas, Nov. 17, 1975.

5. Skylab Mission Report, First Visit, JSC-08414, August 1973. Prepared by Mission Evaluation Team, L. B. Johnson Space Center, Houston, Texas. Section 3.0 Skylab Parasol.

6. Skylab 1/3 Bilevel Strip Chart. Data of CSM RCS and TACS Thrusters ON/OFF Switching from Analog PCM Tapes Numbers Z05-000015 and Z05-000016 (Goldstone and Bermuda telemetry receiving stations) processed and stored in the Data Distribution Center, Lyndon B. Johnson Space Center, Houston, Texas.

7. Jacobs, Stephen and Ballentine, Thomas J. Skylab Parasol Material Evaluation. JSC-09452, NASA TMX-58161, NASA, JSC, Houston, Texas, April 1975.

8. Technical Report. Skylab Saturn Workshop/Orbital Assembly Attitude and Pointing Control System Postflight Performance Evaluation. 80M19007, April 30, 1974. Prepared by the Skylab Guidance and Controls Group, Bendix Corporation/Martin Marietta Aerospace, Denver, Colorado, for the Orbital Analysis Branch, Dynamics and Control Division, Aero-Astrodynamics Laboratory, George C. Marshall Space Flight Center, Huntsville, Alabama. Section 8.1.2 SL-3 Docking.

9. Skylab Program Operational Data Book, Volume IV, Skylab Performance Data, Amendment 53 (C4/25/73) MSC-01549 (Vol. IV), Rev. A, Section 2. Propulsion System. Manned Spacecraft Center, Houston, Texas.

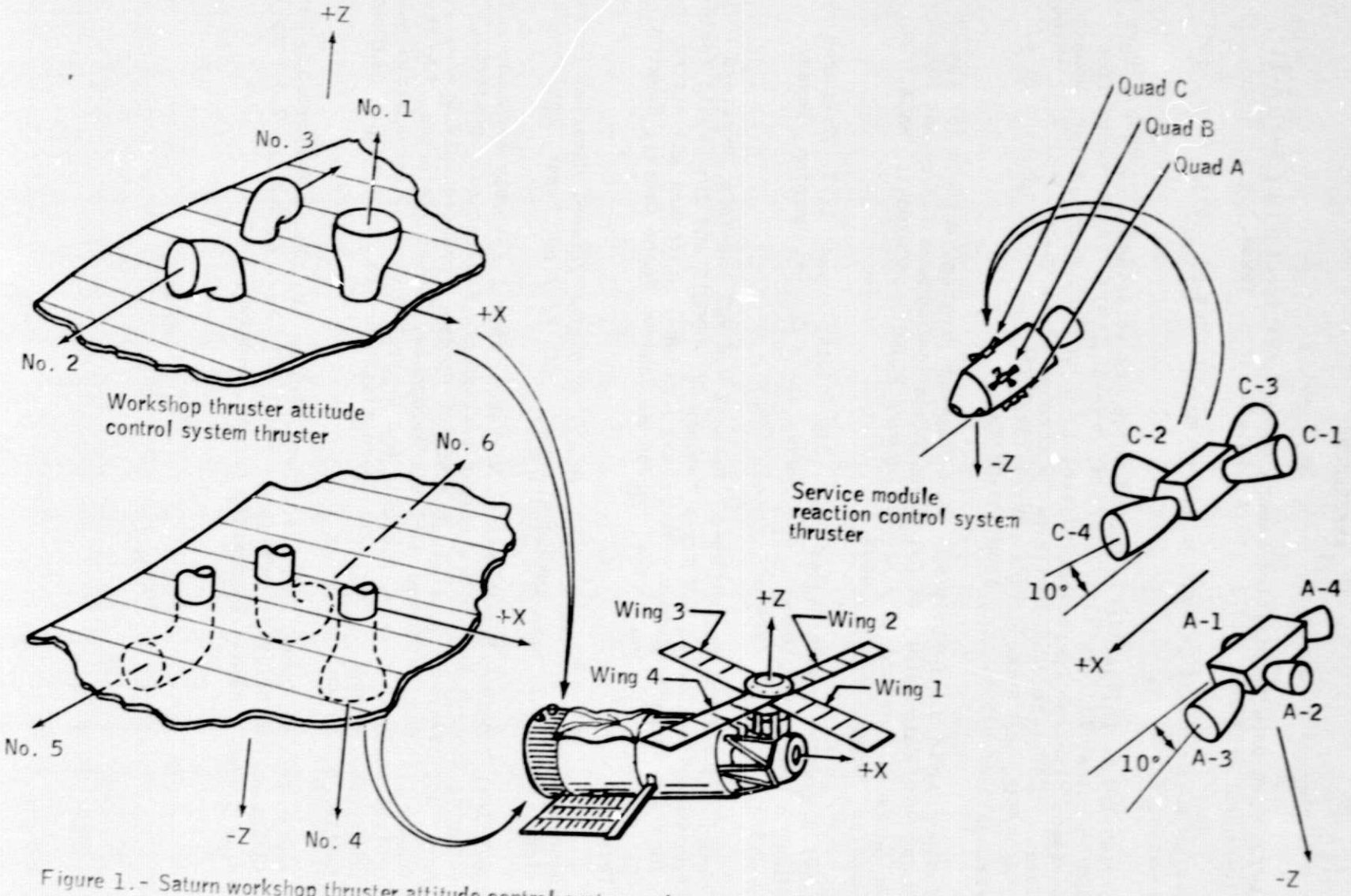

Figure 1.- Saturn workshop thruster attitude control system and service module reaction control system thruster identification.

ORIGINAL PAGE IS
OF POOR QUALITY

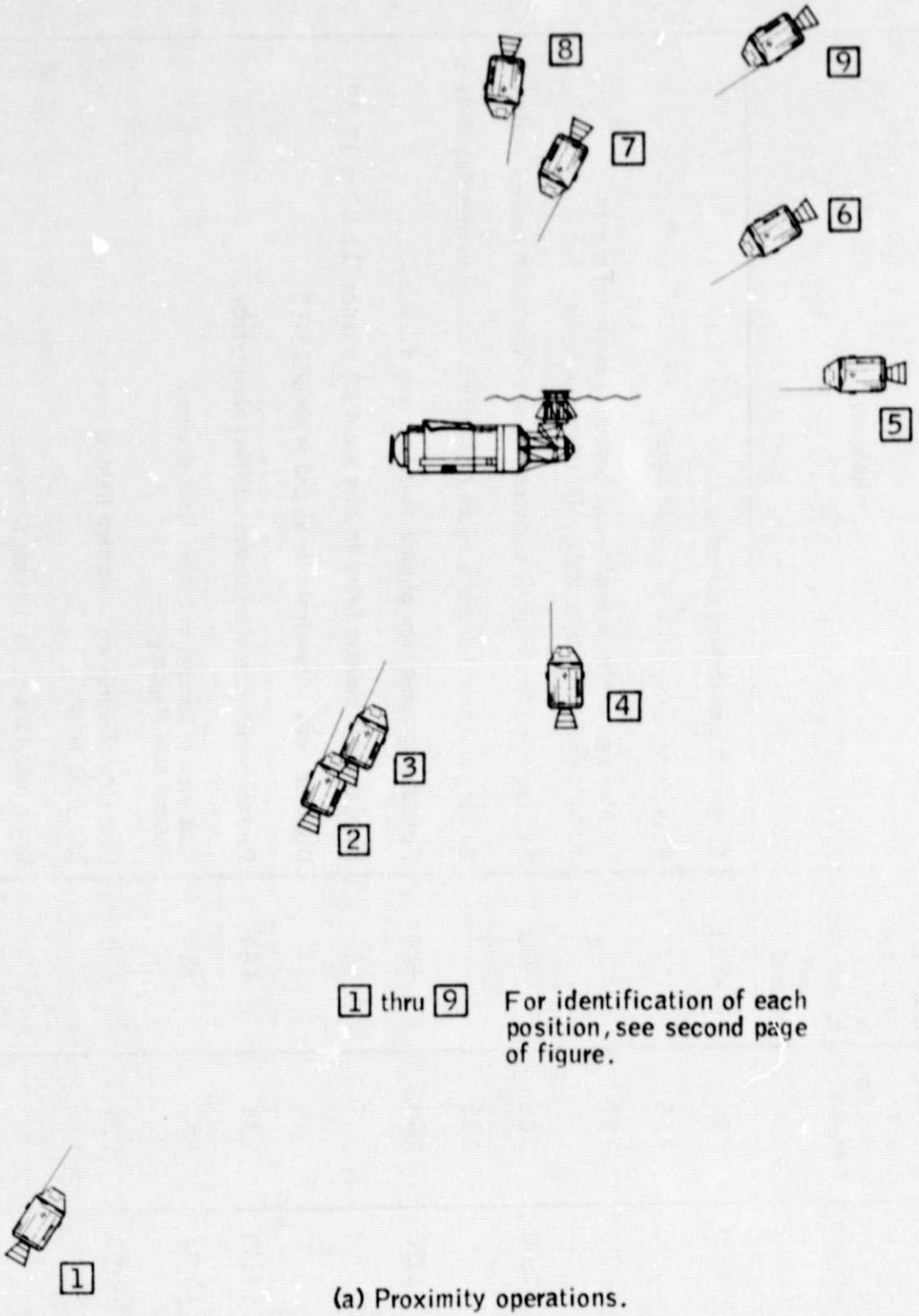

1 thru 9 For identification of each position, see second page of figure.

(a) Proximity operations.

Figure 2.- Pre-docking approach and fly-around on second visit to Skylab.

Position number	Time after 209:19 G.m.t., min:sec	Distance spacecraft camera to workshop X-Axis feet	Approximate angle to spacecraft X-Axis to workshop X-Axis degrees	Remarks
1	4:00	420	-120	Spacecraft approaching workshop.
2	5:45	165	-115	First photographic view of parasol motion.
3	6:00	137	-110	Looking into wardroom window and beginning movement toward multiple docking adapter and Apollo telescope mount.
4	7:00	105	-90	Looking at center of Apollo telescope mount. Spacecraft nearest workshop.
5		126	0	Looking at Apollo telescope mount in direction parallel to workshop X-Axis.
6	11:20	160	+30	First photographic view of parasol motion from +Z side.
				No spacecraft thruster firing data for about $1\frac{1}{2}$ minutes (11:00 to 12:30).
				Decision made to terminate fly around at about 13:15.
7	14:33	134	+64	Parasol motion (flaps) measured utilizing photography.
8	16:03	153	+80	Last view of parasol in camera field of view. Parasol still flapping.
9	19:03	220	+30	Last view of workshop in camera field of view. End of fly around.
				Begin preparations for docking sequence.

(b) Notes for figure 2.

Figure 2.- Concluded.

ORIGINAL PAGE IS
OF POOR QUALITY

Figure 3.- Spacecraft, workshop and parasol during approach and fly-around maneuver.

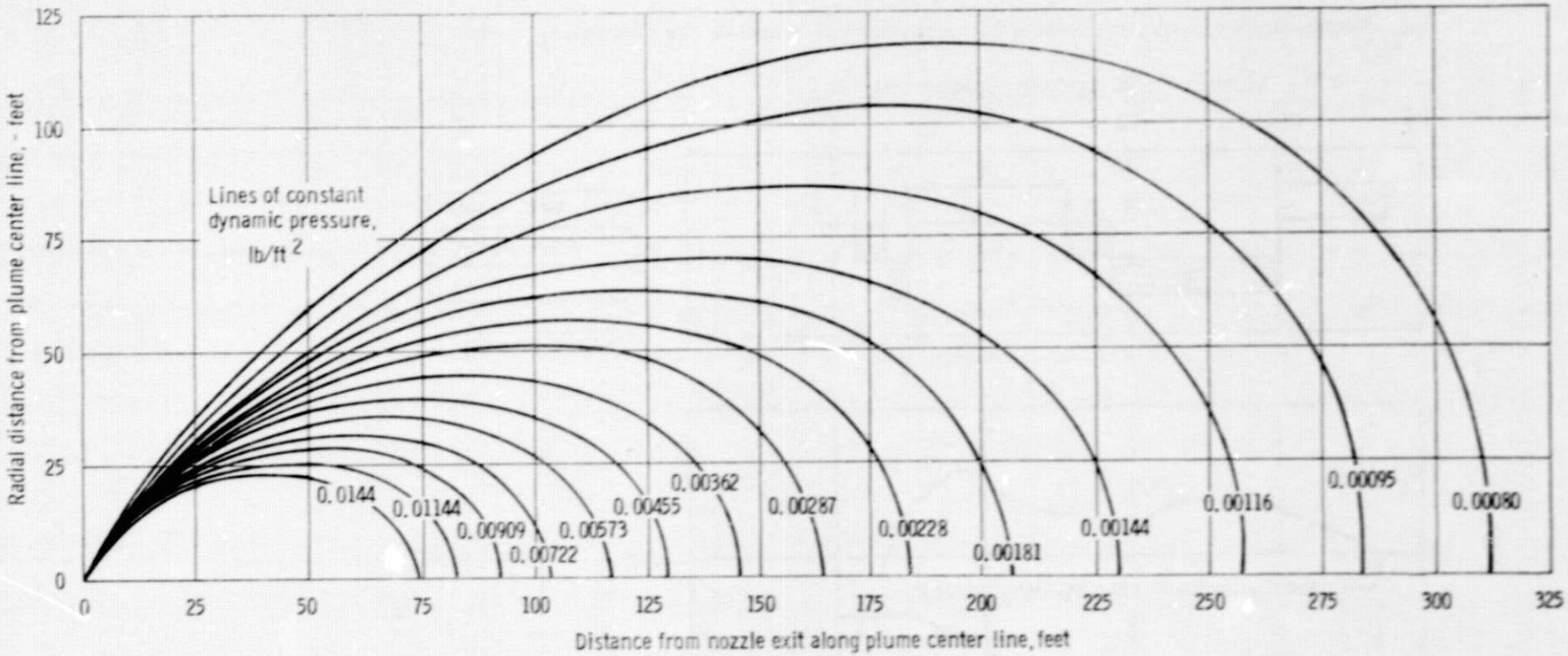

$$q = \frac{\gamma P_0 r_e^2 A_* \left(\frac{\gamma+1}{2}\right)^{-\frac{1}{\gamma-1}}}{2 A_e (\gamma-1)\left(\frac{\gamma+1}{\gamma-1}\right)^{\frac{1}{2}}} \cdot \frac{\cos^{\frac{2}{\gamma-1}}\theta}{r^2 \int_0^{\theta_\ell} \cos^{\frac{2}{\gamma-1}} \frac{\pi\theta}{2\theta_\ell} \sin\theta \, d\theta}$$

- r Distance to given point from nozzle exit
- θ Angle of "r" with plume center line
- q Dynamic pressure
- γ Ratio of specific heats for the propellants
- P_0 Rocket chamber pressure
- r_e Nozzle exit radius
- A_* Nozzle throat area
- A_e Nozzle exit area
- θ_ℓ Limiting turning angle for the gas

Figure 4. - Command and service module reaction control system plume impingement model.

ORIGINAL PAGE IS
OF POOR QUALITY

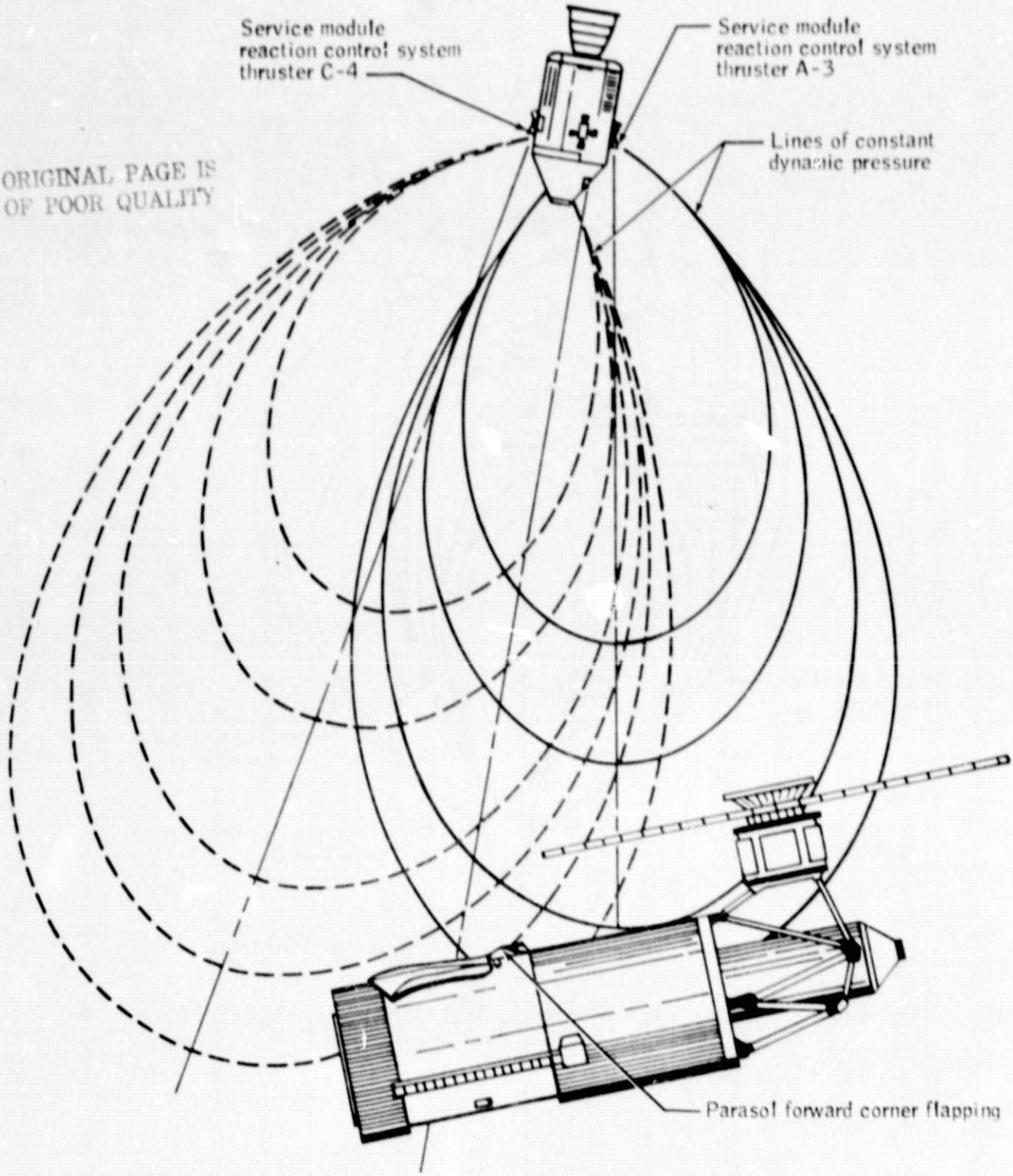

Figure 5.- Workshop parasol in plume impingement model force fields for service module reaction control system thrusters A-3 and C-4 at about 209:19:14.33 G.m.t.

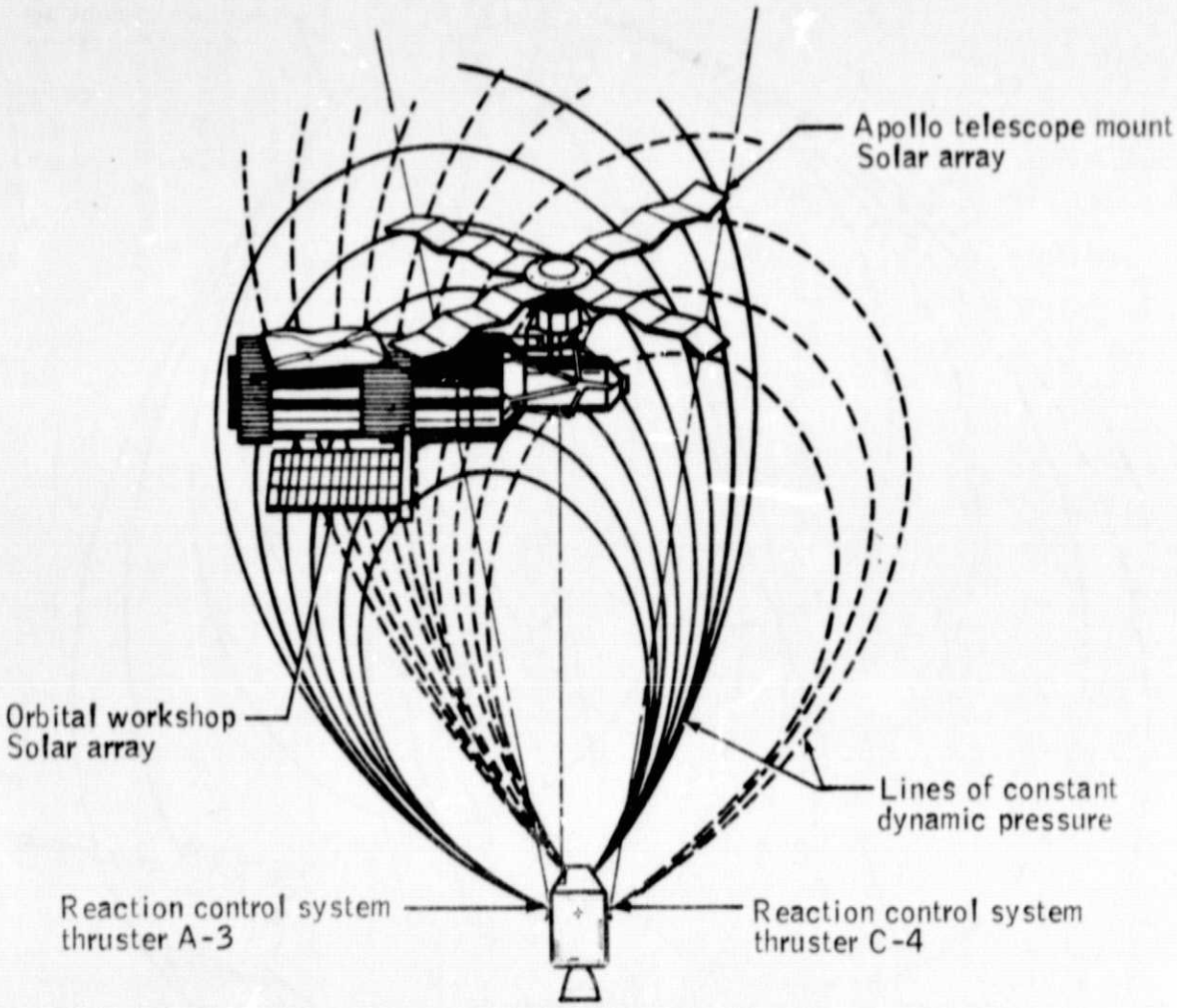

(a) Spacecraft /workshop separation distance of 100 feet.

Figure 6. - Saturn workshop solar arrays in plume impingement model force fields for reaction control system thrusters A-3 and C-4.

ORIGINAL PAGE IS
OF POOR QUALITY

ORIGINAL PAGE IS
OF POOR QUALITY

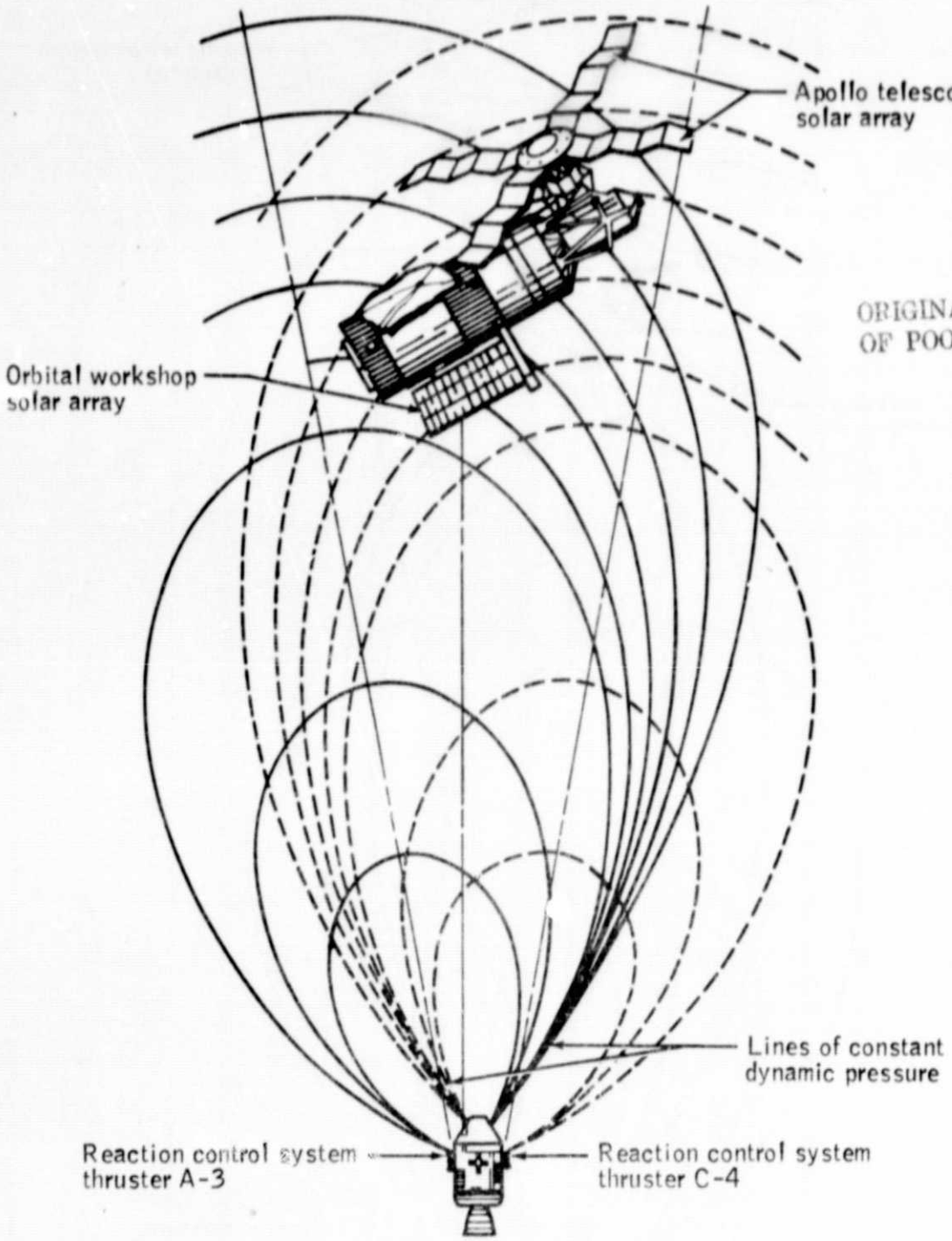

ORIGINAL PAGE IS
OF POOR QUALITY

(b) Spacecraft/workshop separation distance of about 200 feet.

Figure 6.- Continued.

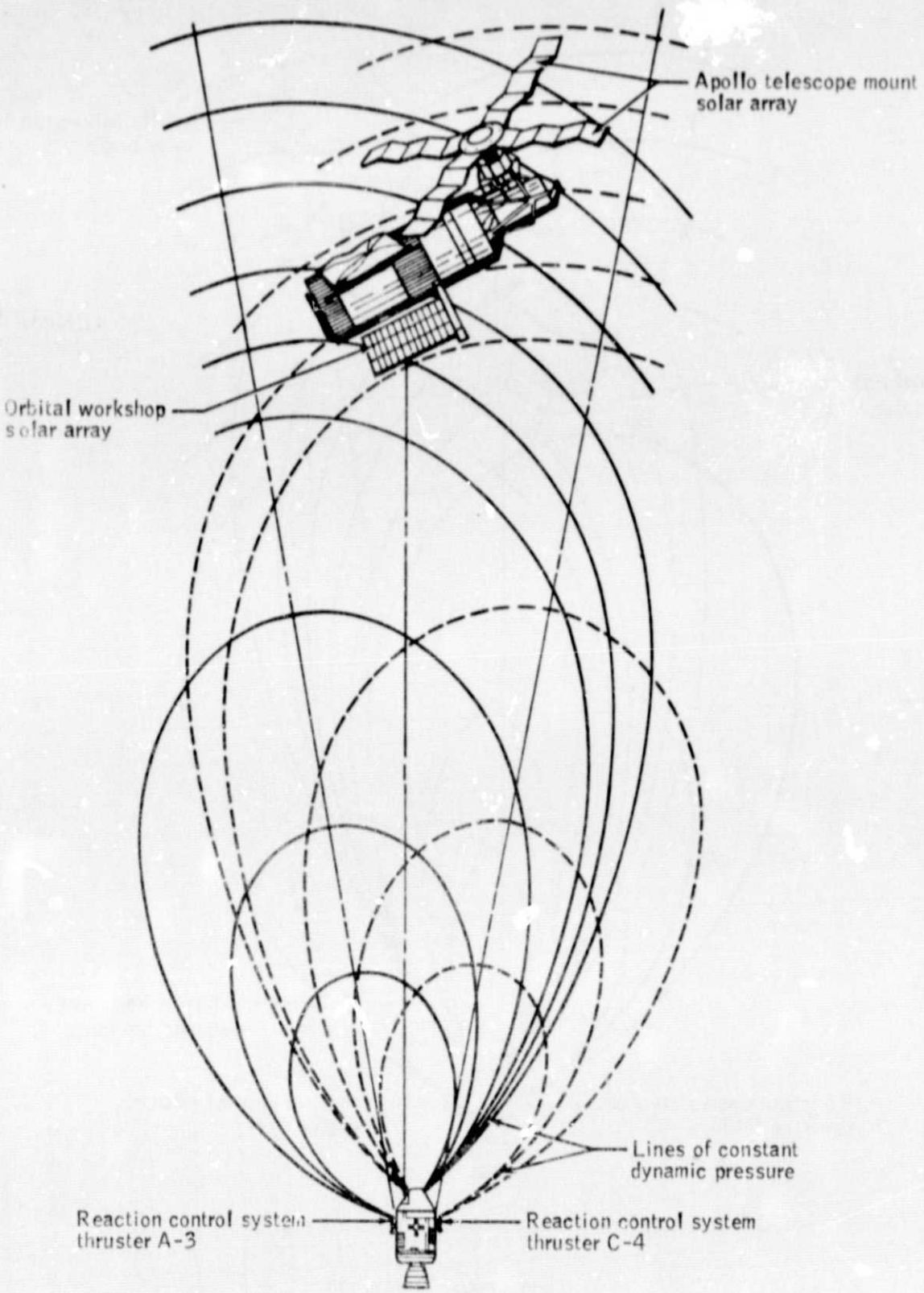

(c) Spacecraft/workshop separation distance of about 265 feet.

Figure 6.- Concluded.

ORIGINAL PAGE IS
OF POOR QUALITY

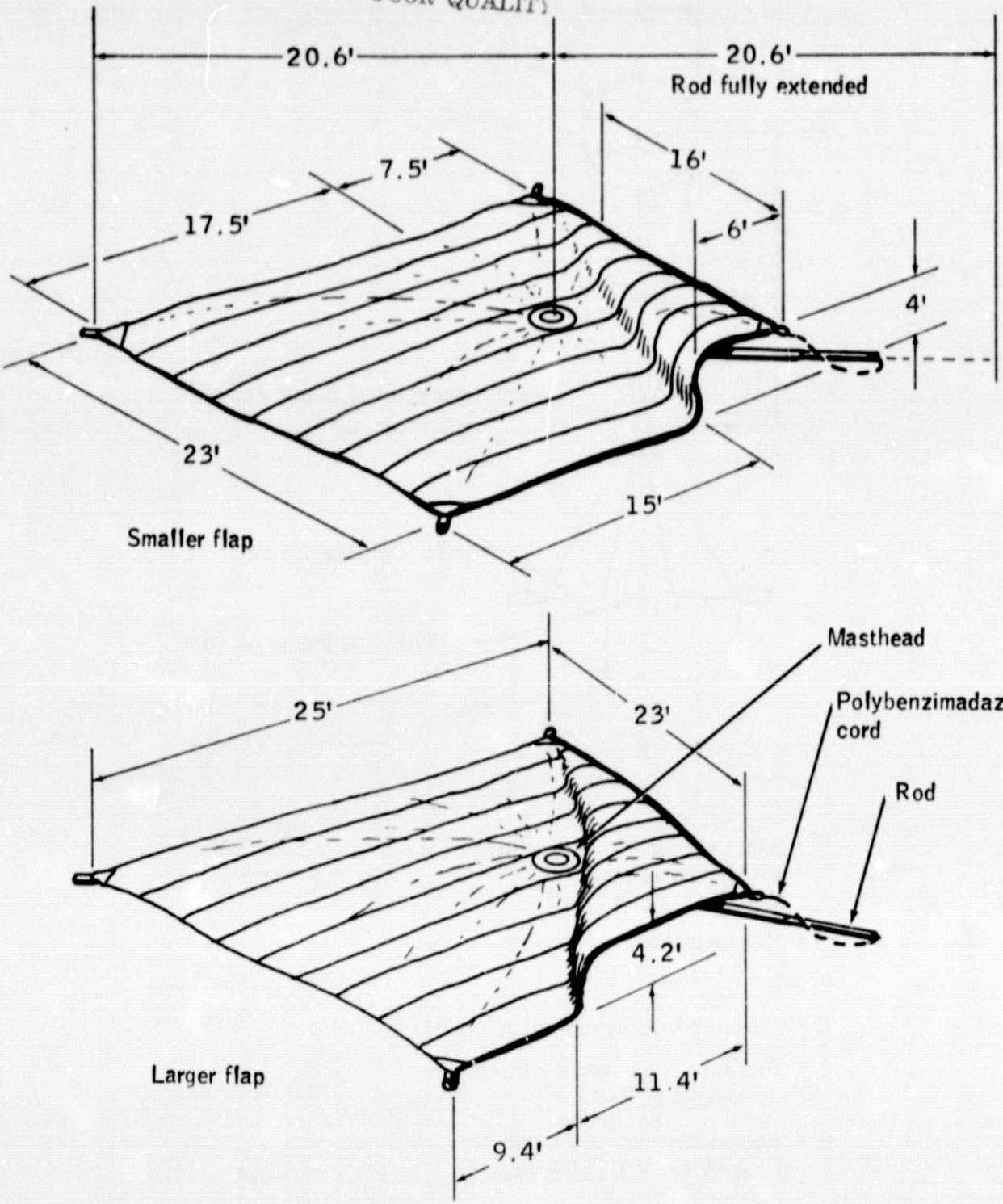

Figure 7.- Saturn workshop parasol at 209:19:14.33 G.m.t.

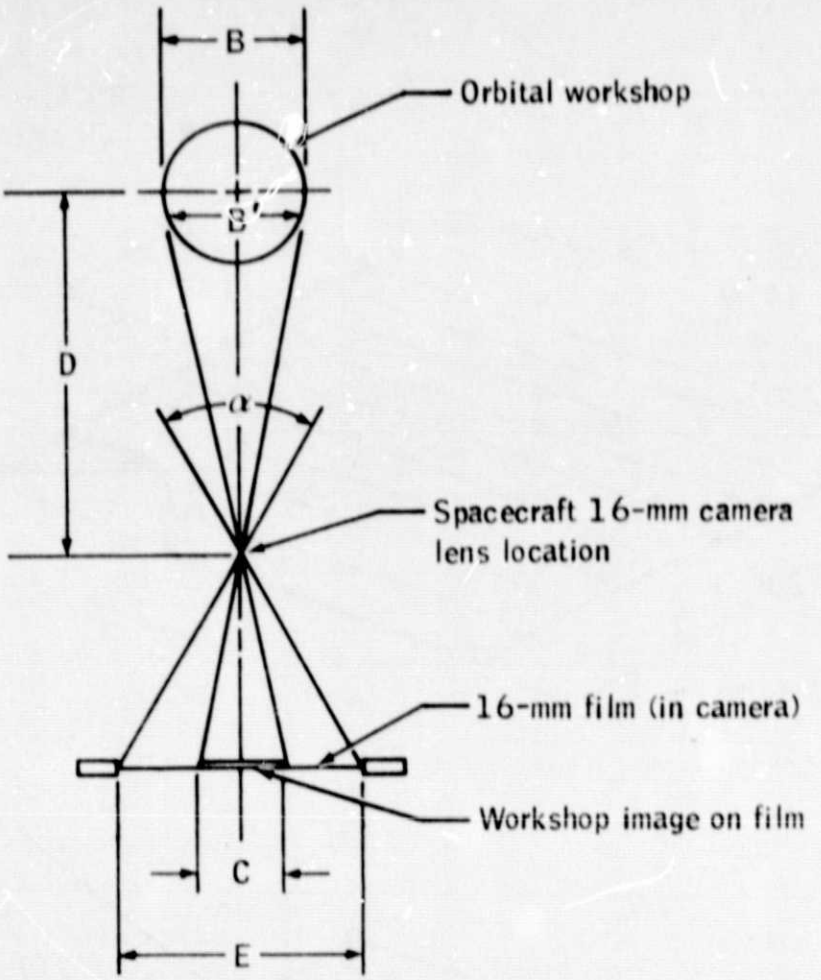

α = Known field-of-view angle of 16-mm camera $23.4^\circ \times 32.6^\circ$

B = Known workshop diameter

$B' \approx B$

C = Measured workshop image on film

D = Distance from spacecraft camera to workshop X-Axis

E = Known 16-mm film frame size 0.295 in. X 0.404 in.

$$\frac{B}{C} = \frac{2D \text{ TAN } \frac{1}{2}\alpha}{E}$$

$$D = \frac{BE}{2C \text{ TAN } \frac{1}{2}\alpha}$$

Figure 8.- Finding workshop-spacecraft separation distances.

ORIGINAL PAGE IS
OF POOR QUALITY

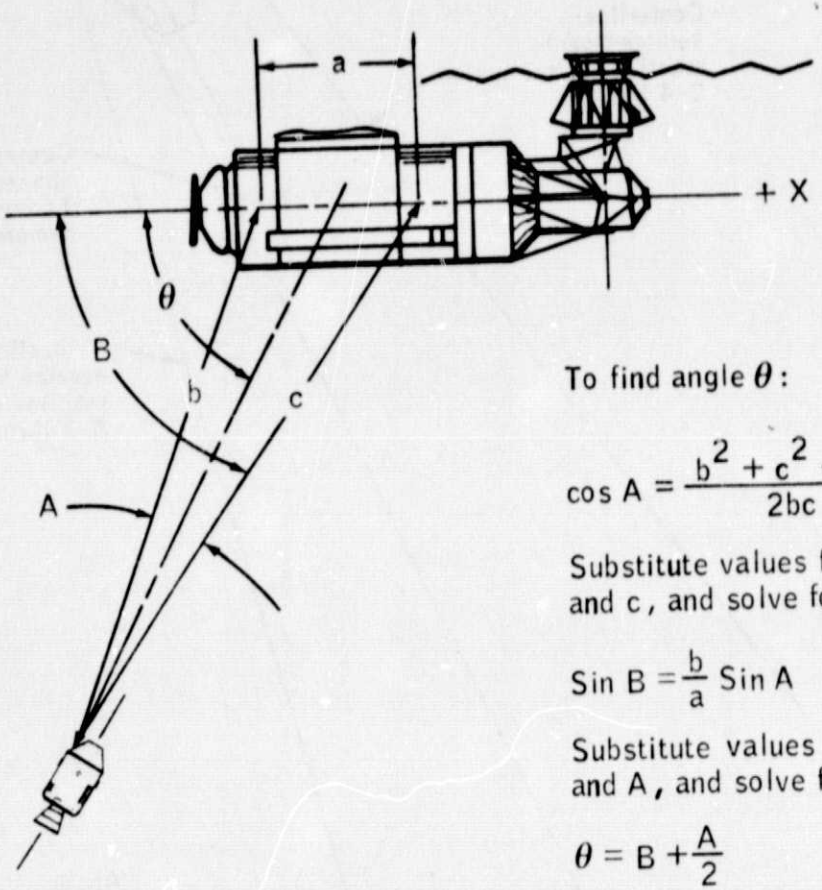

To find angle θ:

$$\cos A = \frac{b^2 + c^2 - a^2}{2bc}$$

Substitute values for a, b, and c, and solve for A

$$\text{Sin } B = \frac{b}{a} \text{ Sin } A$$

Substitute values for a, b, and A, and solve for B.

$$\theta = B + \frac{A}{2}$$

a = Known distance between two selected points on workshop.

b and c = Calculated distances (figure 8) from spacecraft camera to the two selected points on workshop.

θ = Angle of camera centerline with workshop X-Axis.

Figure 9. - Finding attitude orientation angles between the spacecraft and workshop.

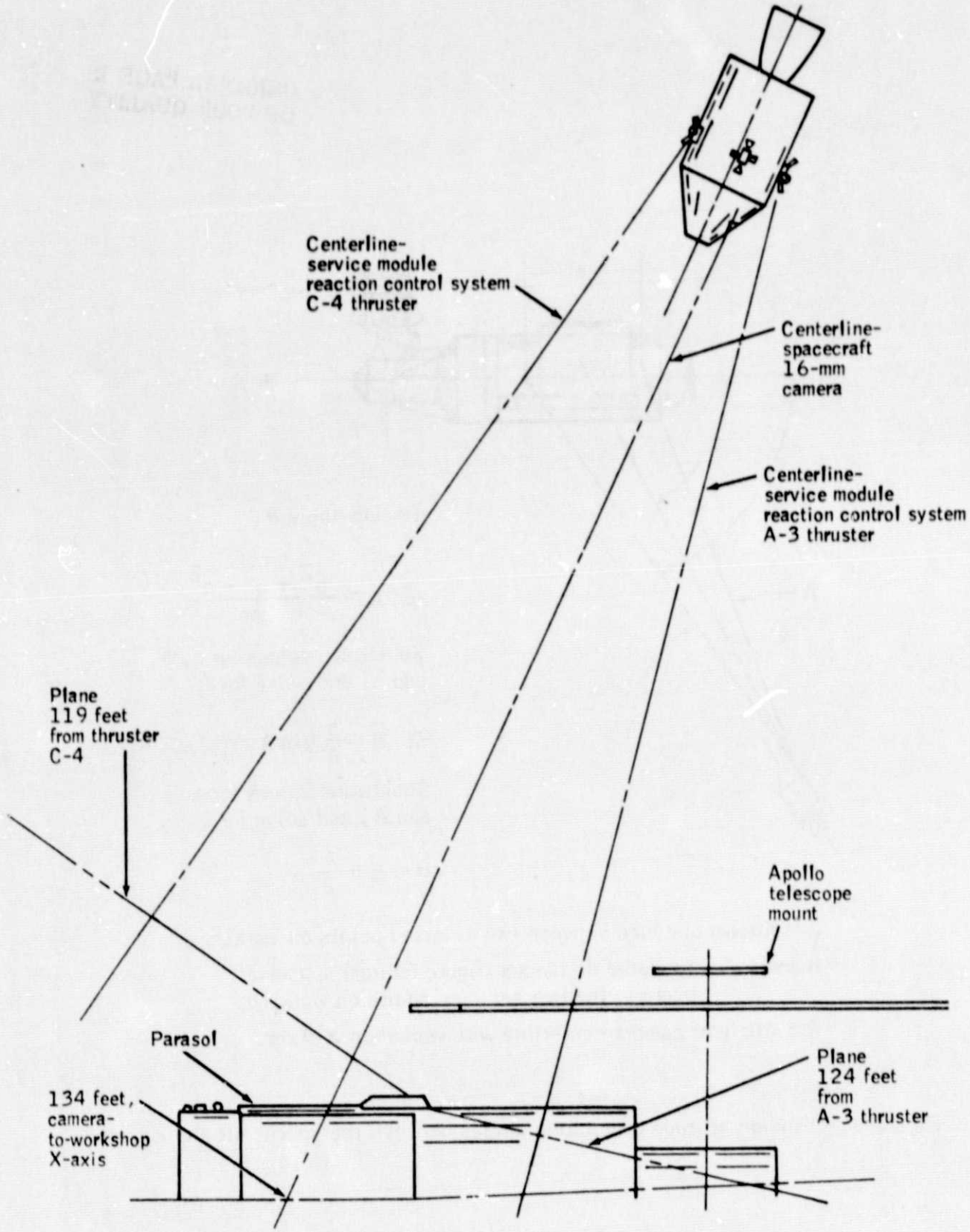

(a) At parasol

Figure 10.-Dynamic pressure.

ORIGINAL PAGE IS
OF POOR QUALITY

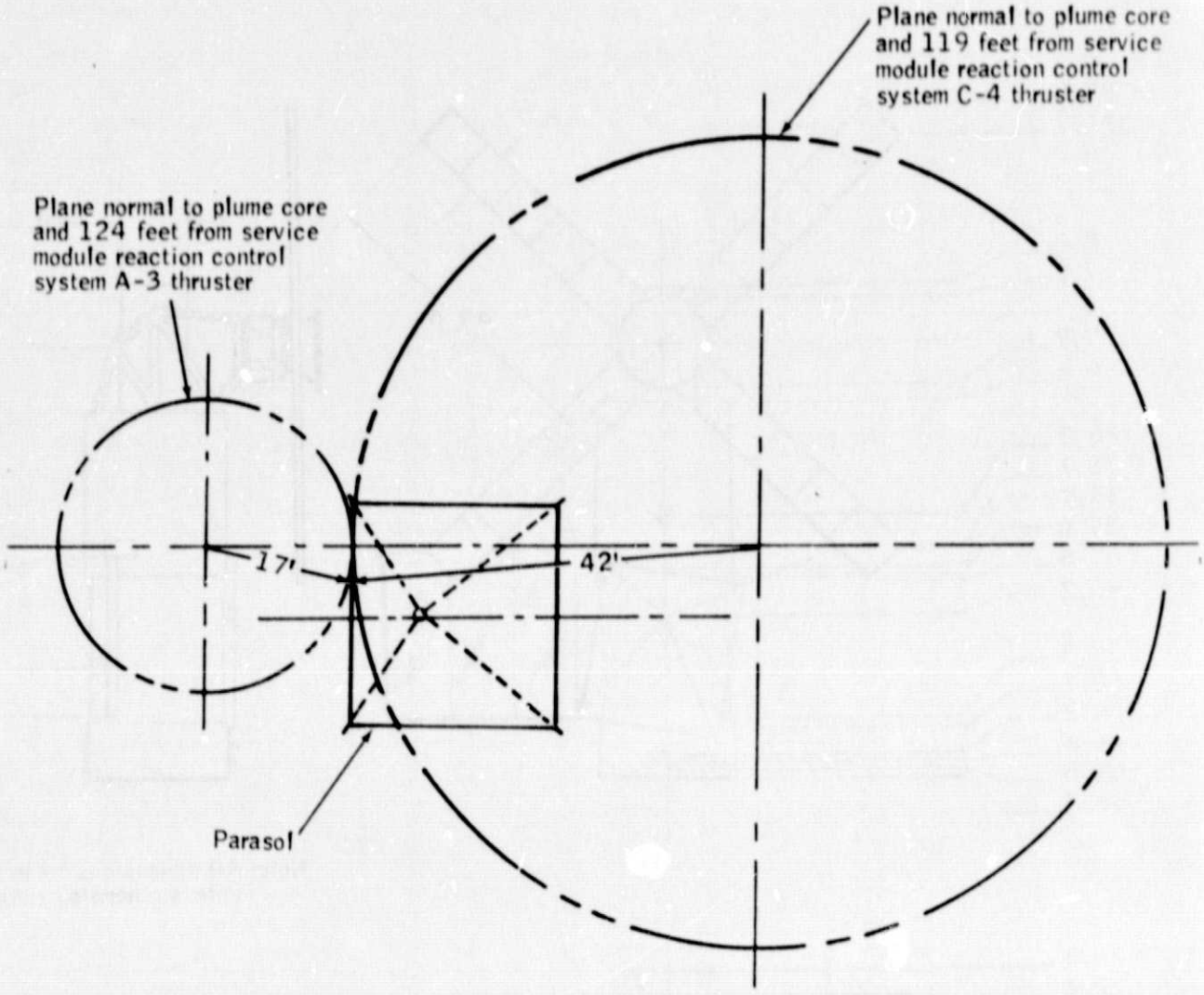

Dynamic pressure-

From A-3 thruster (124 ft. x 17 ft.): 0.00455 lb/ft^2

From C-4 thruster (119 ft. x 42 ft.): 0.00324 lb/ft^2

(b) From plume impingement model

Figure 10.- Concluded.

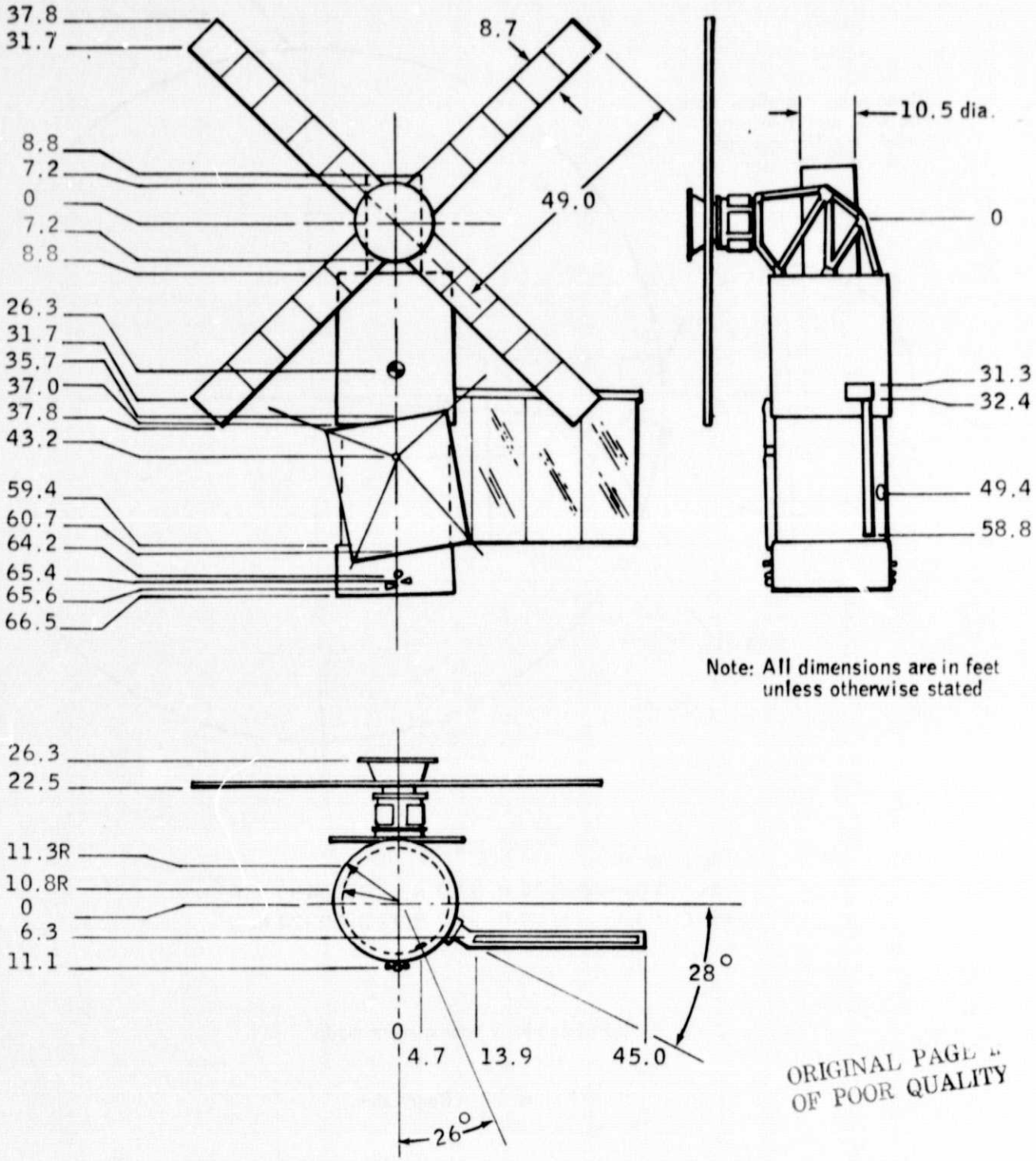

ORIGINAL PAGE IS
OF POOR QUALITY

Figure 11.- Saturn workshop dimensions.

NASA-JSC